FACILITY DESIGN AND MEASUREMENTS OF BISTATIC AND MONOSTATIC REFLECTIVITY OF X, KU, KA, AND W-BAND FREQUENCIES OVER SAND TERRAIN

Brenda L. Matkin
James H. Mullins
Missile Guidance Directorate
Aviation and Missile Research, Development, and Engineering Center

Tommy Ferster
System Simulation and Development Directorate
Aviation and Missile Research, Development, and Engineering Center

and

Perry Vanderford
Simulation Technologies
P. O. Box 7009
Huntsville, AL 35807

February 2002

DESTRUCTION NOTICE

DISCLAIMER

TRADE NAMES

REPORT DOCUMENTATION PAGE

1. AGENCY USE ONLY	2. REPORT DATE	3. REPORT TYPE AND DATES COVERED
	February 2002	Final

4. TITLE AND SUBTITLE
Facility Design and Measurements of Bistatic and Monostatic
Reflectivity of X, Ku, Ka, and W-Band Frequencies Over Sand Terrain

5. FUNDING NUMBERS

6. AUTHOR(S)
Brenda L. Matkin, James H. Mullins, Tommy Ferster, Perry Vanderford

7. PERFORMING ORGANIZATION NAME(S) AND ADDRESS(ES)

Commander, U. S. Army Aviation and Missile Command
ATTN: AMSAM-RD-MG-RF
Redstone Arsenal, AL 35898-5000

8. PERFORMING ORGANIZATION REPORT NUMBER

TR-RD-MG-01-38

9. SPONSORING / MONITORING AGENCY NAME(S) AND ADDRESS(ES)

10. SPONSORING / MONITORING AGENCY REPORT NUMBER

11. SUPPLEMENTARY NOTES

12a. DISTRIBUTION / AVAILABILITY STATEMENT
Approved for public release; Distribution is unlimited

12b. DISTRIBUTION CODE

A

13. ABSTRACT *(Maximum 200 Words)*

This report provides an overview of an X, Ku, Ka, and W-Band monostatic and bistatic measurement facility in the Aviation and Missile research, Development, and Engineering Center (AMRDEC) at Redstone Arsenal, Alabama. The data collection includes both on-axis (zero degrees) and off-axis (10 and 30 degrees) measurements of the bistatic reflectivity response. The instrumentation design for the data collection will be briefly described. The calibration processes and the data collection methodologies for monostatic and bistatic measurements will be discussed. A summary of the reflectivity results from smooth sand terrain will be presented. This work has application to tactical missile systems that must complete their engagements at low altitudes in a clutter environment.

14. SUBJECT TERMS

Bistatic, Monostatic, Reflectivity, X-Band, Ku-Band, Ka-Band, W-Band, Anechocic Chamber, Instrumentation

15. NUMBER OF PAGES
31

16. PRICE CODE

17. SECURITY CLASSIFICATION OF REPORT	18. SECURITY CLASSIFICATION OF THIS PAGE	19. SECURITY CLASSIFICATION OF ABSTRACT	20. LIMITATION OF ABSTRACT
UNCLASSIFIED	UNCLASSIFIED	UNCLASSIFIED	SAR

NSN 7540-01-280-5500

Standard Form 298 (Rev. 2-89)
Prescribed by ANSI Std. Z39-18
298-102

ACKNOWLEDGEMENTS

EXECUTIVE SUMMARY

Data that realistically represents the phenomenology of monostatic and bistatic reflectivity is essential to the design of radar systems intended to sense land based targets and low flying aircraft. A large database exists describing the response of X-Band monostatic reflectivity, and limited data is available for X-Band bistatic reflectivity. However, there is little data in the literature describing bistatic reflectivity at Ku-Band or at millimeter wave bands. Radar designers often resort to either scaling, or using directly, the bistatic reflectivity of X-Band to model this environment at the other frequencies. A need exists to further characterize clutter phenomenology in order to design and project the performance of current and future systems.

This report provides an overview of an X, Ku, Ka, and W-Band monostatic and bistatic measurement facility in the Aviation and Missile Research, Development and Engineering Center (AMRDEC) at Redstone Arsenal Alabama. The data collection includes both on-axis (zero degrees) and off-axis (10 and 30 degrees) measurements of the bistatic reflectivity response. The instrumentation design for the data collection will be briefly described. The calibration processes and the data collection methodologies for monostatic and bistatic measurements will be discussed. A summary of the reflectivity results from smooth sand terrain will be presented. This work has application to tactical missile systems that must complete their engagements at low altitudes in a clutter environment.

TABLE OF CONTENTS

LIST OF ILLUSTRATIONS

LIST OF TABLES

I. INTRODUCTION

A Bistatic Reflectivity Measurement Facility (BRMF) was developed by the Missile Guidance and Systems Simulation and Development Directorates at Redstone Arsenal. This facility was used to measure the bistatic reflectivity of sand, and it is planned to measure the reflectivity of other terrain types in the future. It is of interest to the Radio Frequency (RF) seeker developer to understand how bistatic forward returns from the target could impact the seeker detection and track. Particularly, smart weapons engaging ground-based targets and land combat missiles engaging either ground based or low altitude targets could be adversely affected by a strong ground bounce return, multipath, or jamming. Therefore, it was desired to characterize a set of bistatic returns, beginning with smooth sand, in order to better understand this phenomenon. Figure 1 illustrates the bistatic signal geometry [1].
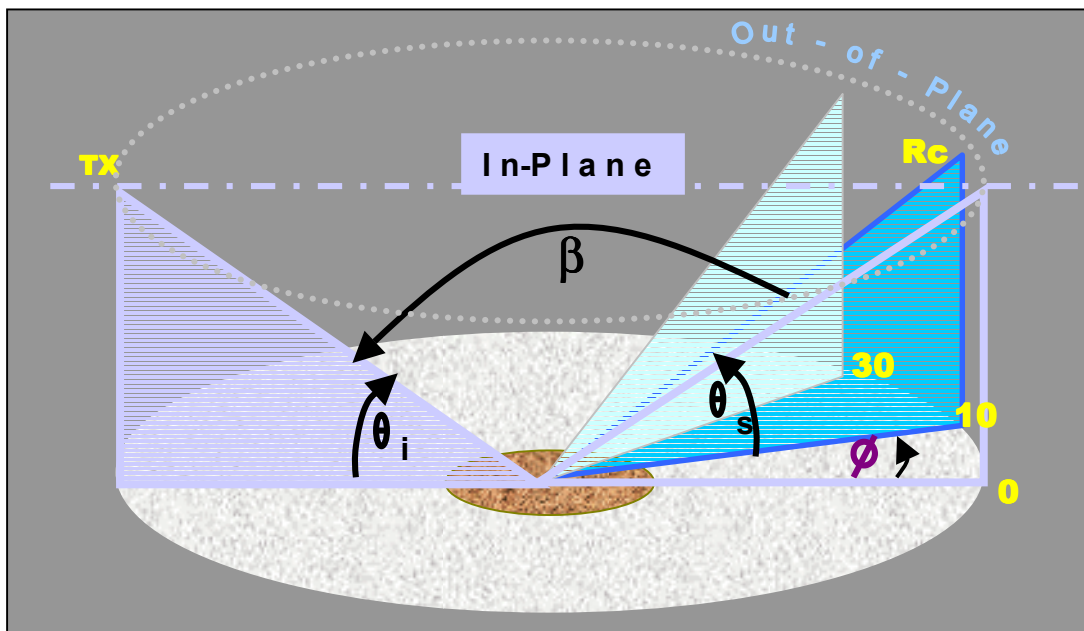
Figure 1. Illustration of Bistatic Signal Geometry

The bistatic angles shown are defined as

θ_I = incident angle on signal on the terrain
θ_s = scattering angle of reflected signal
ϕ = out-of-plane angle
β = angle between incident and scattered signal paths

The in-plane or 'specular' bistatic geometry occurs when the transmitter and receiver are at the same depression angle and are in-plane at 0 degrees. Generally, if the receiver antenna is out-of-plane at some other angle, then the bistatic signal from the ground bounce will decrease in amplitude and have a diffuse character. The out-of-plane angles examined for this measurement program were 10 and 30 degrees.

II. MEASUREMENT FACILITY

A. Facility Overview

The BRMF is illustrated in Figure 2, and in the photograph of Figure 3. The overall wiring relationships are shown in Figure 4. The facility utilizes an anechoic chamber that measures 35 by 28 feet in length and width and has a height of 35 feet. The chamber is equipped with a combination of 4, 12, 24, and 48-inch anechoic material on the walls and ceiling and parts of the floor. In the vicinity of the turntable, 8-inch anechoic material is used to reduce the interference from the higher millimeter wave frequencies. The spectral purity of the chamber was measured prior to the addition of the turntable and towers by measuring the bistatic response of a 6-foot diameter circular patch of high frequency anechoic material. This measurement was repeated after the addition of the turntable and towers. In both measurements the response was about -30 dBsm.
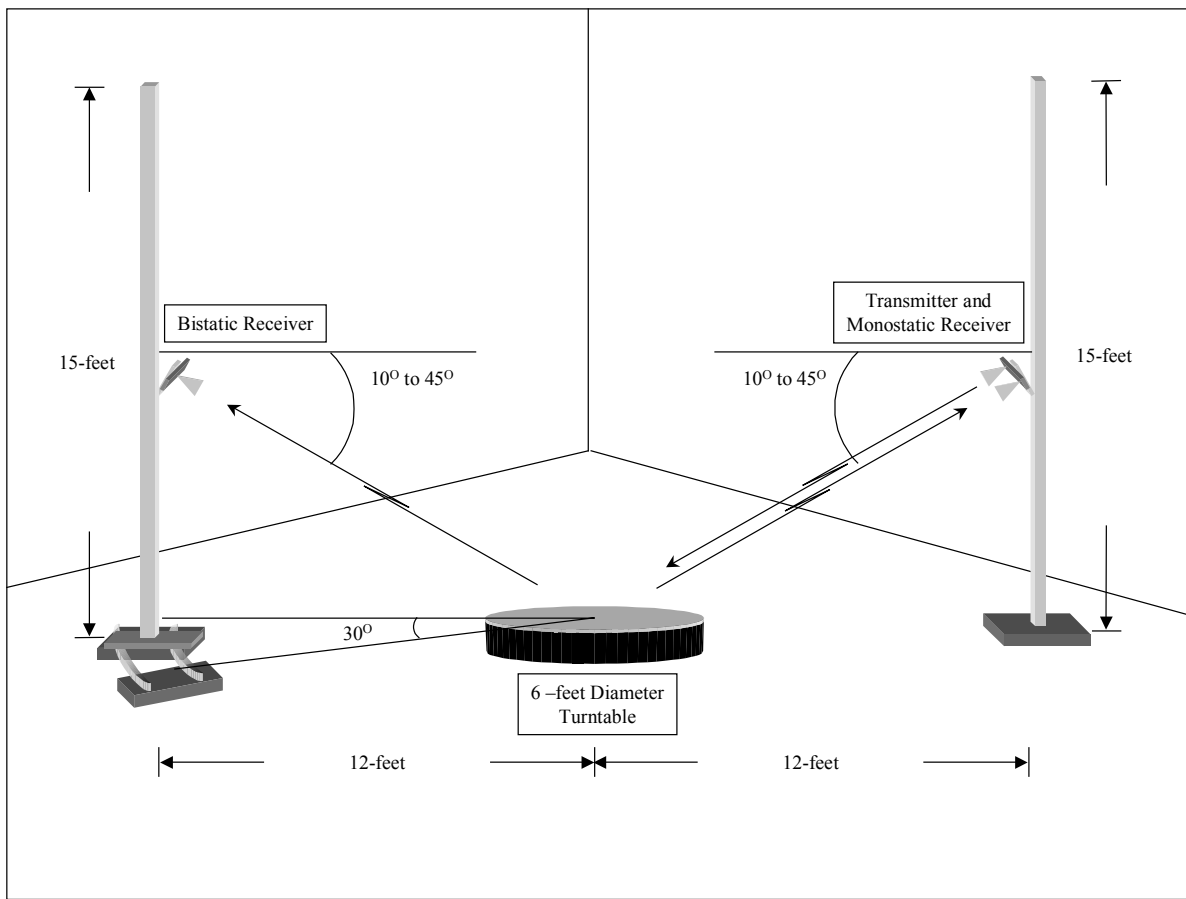
Figure 2. Bistatic Reflectivity Measurement Facility Diagram

A turntable was fabricated to locate targets and terrain samples to be measured. The turntable is 6 feet in diameter, supports weight in excess of 1000 pounds, and can be

programmed to rotate continuously through a full 360 degrees, or to rotate and stop at any angular position within 360 degrees. Additionally, the turntable can be programmed to continuously step and pause at selected angular increments. The turntable supports rotation rates from 0.09 to 1 RPM; i.e., from about 0.6 to 6 degrees per second. The turntable is controlled by a remote panel that is located in an adjacent instrumentation room. The turntable rotation capability provides for the collection of bistatic and monostatic target reflectivity (signatures) over 360 degrees of aspect. Additionally, it supports the collection of Inverse Synthetic Aperture Radar (ISAR) data to provide both range and cross-range target signatures. This capability also provides for statistical relevance in terrain reflectivity measurements. Some general specifications of the turntable are given in Table 1.
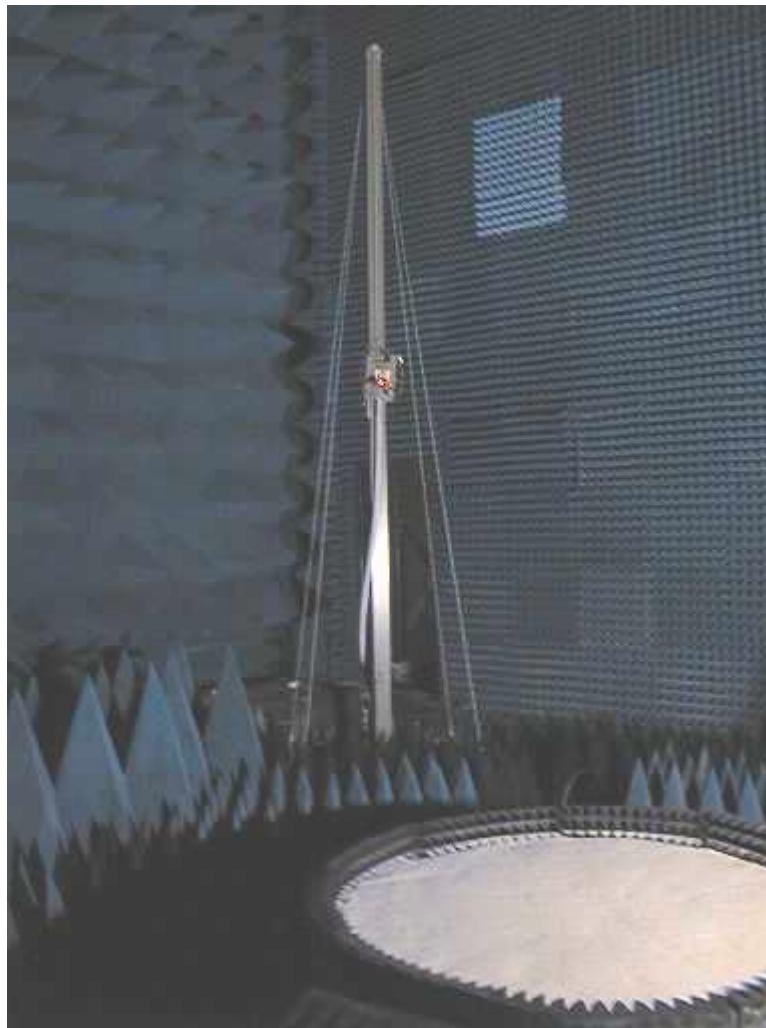
Figure 3. Photograph of the Chamber Turntable and Transmit Tower

The turntable top is constructed of steel. Targets to be measured and which are of a size compatible with the turntable, can be placed on anechoic material on top of the turntable. Terrain samples to be measured are located in a circular wooden container, which is 6 feet in

diameter. It covers the entire top of the turntable and height of the sides is 6 inches. This container is constructed completely of wood and plastic fasteners and contains no metal parts. Anechoic material is located around the sides of the turntable and sample container to reduce reflections from these objects.

Table 1. Specifications for the Turntable and Controller

Weight Handling Capability	1200 lb
Rotation Speed	0.09 to 1.0 rpm
Rotation Angle Increment Size	0.5 to 19.0 degrees
Pause Time At Increment	0.01 to 20 sec

Towers for the transmitters and receivers were constructed of Extren fiberglass. The transmitter and receiver elevators are also made of Extren fiberglass. The towers are located 12 feet from the center of the terrain turntable. One tower supports the bistatic receiver while the other supports the transmitter and monostatic receiver. The towers are 15 feet in height. The transmitter and receivers are mounted to elevators, platforms that are adjustable in height via a pulley mechanism, that allows for positioning the elevators in height along the tower. Heights of 2 to 12 feet are obtainable to support independent adjustments in incidence and reflection angles from 10 to 45 degrees. Additionally, the receiver tower can be positioned from a bistatic in-plane position of 0-degrees up to 30 degrees out of plane position. Currently, the transmitters and receivers are adjustable over depression angles of 15 to 45 degrees in 5-degree steps by changing the height of the antennas on the antenna masks.

The final micro/millimeter wave power amplifiers are located on the tower elevators. Synchronization of the transmitter and receivers are provided by instrumentation located in the instrumentation room, and the synchronization signals are routed from the instrumentation room to the transmitter and receivers via coaxial cables located beneath the anechoic material. The tower elevators also include a visible laser that is boresighted with the transmitter and receiver antennas to aid in the pointing of the RF beams at the turntable and calibration sources. When tests are performed at Ka and W-Band, the tower RF instrumentation includes the basic building blocks for the Ka and W-Band transmitters and receivers. These basic building blocks are the Aviation Missile Command (AMCOM) Hardware-In-the-Loop (HWIL) upconverter modules used in testing of Ka and W-Band seekers within the AMRDEC Systems Simulation and Development Directorate.

The adjacent instrumentation room houses the turntable control panel, the RF instrumentation for generation of basic X and Ku-Band RF signals and to provide the synchronization signals, and instrumentation for the collection and initial reduction of the reflectivity data.

The instrumentation includes an HP8510C network analyzer with an HP 8517B S-Parameter Test Set, HP8340B and HP83650A Signal Generators, power splitters, amplifiers,

attenuators, and isolators as needed to provide energy at the four RF frequencies used in testing. The data is routed from the bistatic and monostatic receivers to the network analyzer and from the network analyzer to a personal computer for collection and initial analysis.
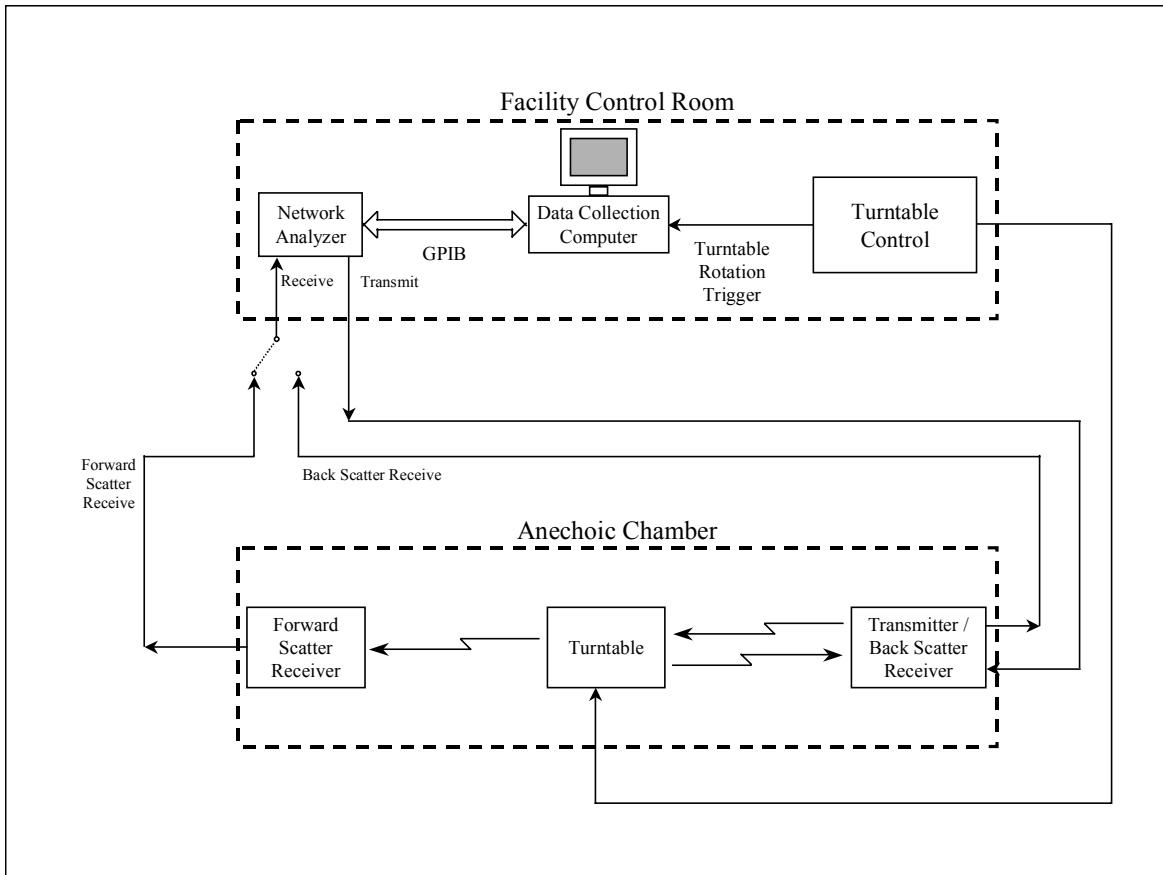
Figure 4. Bistatic Reflectivity Measurement Wiring Relationships

B. RF Transmit and Receive Chains

The RF transmit and receive chains provide for the generation and synchronized reception of RF energy at X, Ku, Ka, and W-Bands. It will be seen in the following discussion that the X and Ku-Band chains use signals directly generated by HP signal sources as the basis for the RF energy. The Ka and W-Band chains use signals generated by HP signal sources as inputs to the HWIL upconverter modules as a basis for providing RF energy.

1. X-Band Transmit and Receive Chain

The X-Band transmit and receive chain is shown in conceptual form as Figure 5. The figure shows that the HP8340B provides an RF signal of 8-12 GHz (on the 10 GHz Reference Line) to the HP8501C vector network analyzer/S-parameter test set (HP8510C/HP 8517) combination. The RF signal is then routed to the transmitter located on the transmitter tower via coaxial cables. The transmitter antenna then directs the energy to the target or terrain sample located on the turntable where it is either absorbed or reflected by forward and backward

5

scattering. The antennas used in the measurements are the same as those used in the Ku-Band setup and have a 70 percent gain of 20 dB and beamwidth of 30.5 degrees at this frequency.

In the bistatic collection mode, the bistatic receive chain is selected and the forward scattered energy is received by the bistatic receiver antenna (via the 10 GHz line) where it is then routed via the 10 GHz bistatic line back through coaxial cables to the HP8510C vector network analyzer/S-parameter test set combination. The vector analyzer receives the signal and compares to the signal provided by the signal generator measuring the relative amplitude of the transmitted and received signals and comparing the collected data to calibration levels that are stored within the network analyzer. This data is routed to the personal computer via a General-Purpose-Interface-Bus (GPIB) for collection and analysis.

In the monostatic collection mode, the monostatic receive chain is selected and the back scattered energy is received by the monostatic receiver antenna where it is then routed (via the 10 GHz line) back through coaxial cables to the HP8510C vector analyzer/S-parameter test set combination. As for the bistatic mode, the network analyzer receives the signal and compares it to the signal provided by the signal generator measuring the relative amplitude of the transmitted and received signals and comparing the collected data to calibration levels which are stored within the network analyzer. Again, this data is routed to the personal computer via a GPIB for collection and analysis.
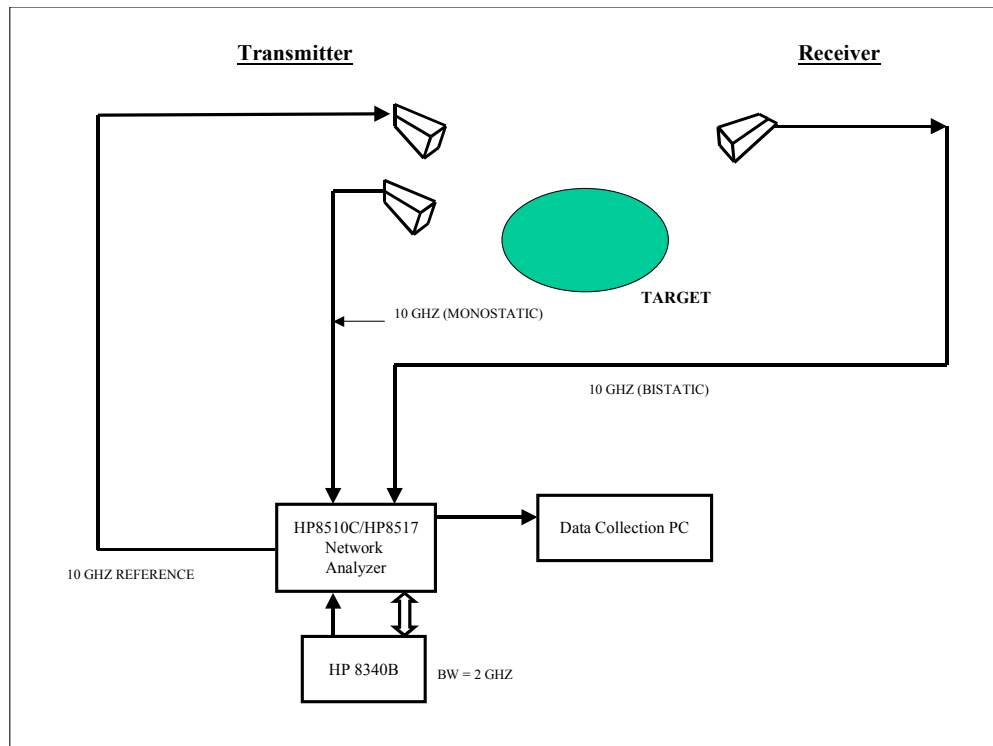
Figure 5. X-Band Measurement Instrumentation Overview

2.   Ku-Band Transmit and Receive Chains

The Ku-Band chains are identical to the X-Band chain with the exception that the HP8340B signal generator provides a basic signal at 14-18 GHz versus the 8-12 GHz signal provided in the X-Band chain. The antennas used in the measurements are the same as those used in the X-Band setup and have a 70 percent gain of 20 dB and beamwidth of 20.5 degrees at this frequency.

3.   Ka-Band Transmit and Receive Chains

The Ka-Band Transmit and Receive Chains are shown in conceptual form as Figure 6. In this realization, the circuit uses Systems Simulation HWIL upconverter modules located on the tower mounted transmitters and receivers as basic building blocks in the generation of Ka-Band energy.
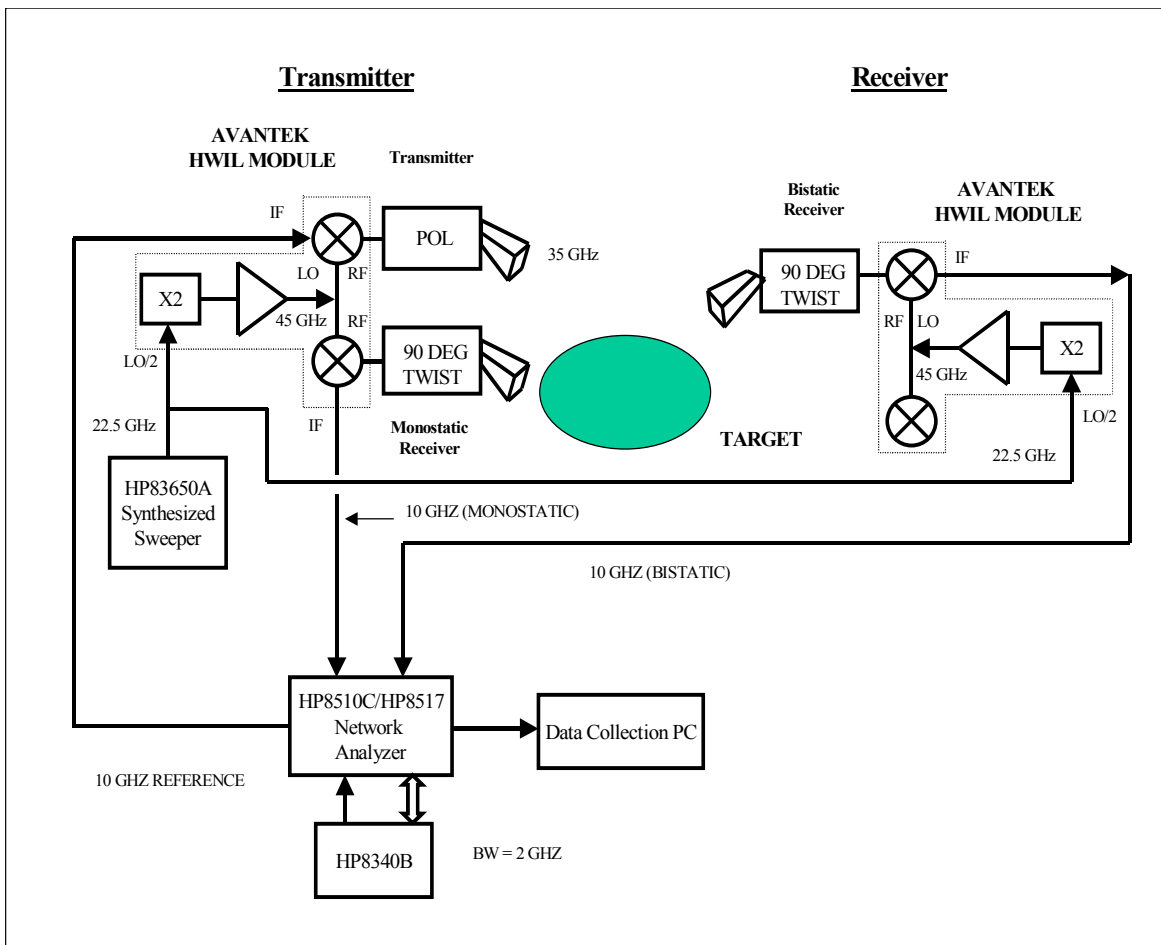
Figure 6. Ka-Band Measurement Instrumentation Overview

The Ka-Band HWIL module, shown in Figure 6, is provided by AVANTEK and includes functions to double the frequency of and amplify a signal applied to the Local Oscillator (LO) at the center port. The module then mixes this LO signal with Intermediate-Frequency (IF)

signals applied at the outer input ports. The output of this module is a signal at frequencies which is the difference between two times the frequency of the LO signal and the IF signal. For the Ka-Band transmit function, a 22.5 GHz signal is applied to the LO port and an 8-12 GHz signal is applied to the IF port of the HWIL module. By subtracting the frequency of the IF signal from two times the frequency of the LO signal, the HWIL module utilizes the LO and IF input to provide a 33-37 GHz RF signal at the transmitter RF output port.

In the receive mode, the HWIL upconverter module operates reciprocally where the 22.5 GHz signal is applied to the LO port and the Ka-Band signal (33-37 GHz) is applied to one of the RF ports. The RF input signal is provided by the forward-scattered energy (for bistatic receive) or by the back-scattered energy (for monostatic receive.) The HWIL upconverter module subtracts, when performing as a downconverter, the frequency of the Ka-Band signal received at the RF port from two times the frequency of the LO signal (22.5 GHz) resulting in an 8-12 GHz IF data output signal. Some specifications of the AVANTEK Ka-Band upconverters are shown in Table 2.

Table 2. Specifications of the AVANTEK HWIL Ka-Band Upconverter

Operating Frequency	
LO/2	20 +/- 2 GHz
IF	10.00 +/- 1 GHz
RF	34.00 +/- 4 GHz
Maximum Conversion Loss	9 dB
Output Compression	1 dB Maximum, with -5 dBm IF Input

The module performed well with an LO input signal of 22.5 GHz and even though the IF bandwidth was specified to be 2 GHz, the upconverter modules were shown to operate over a 4 GHz IF bandwidth.

4.   W-Band Transmit and Receive Chains

W-Band Transmit and Receive Chains are shown in conceptual form as Figure 7. The W-band chains are similar to the Ka-Band chains in that upconverter modules are implemented as basic building blocks to produce the desired RF signal.

The W-Band HWIL upconverter module is produced by SPACEK and as shown in detail in Figure 7, operates similarly to the AVANTEK upconverter modules as described in the previous section. The differences in the upconverters are the LO and RF operating frequencies. The W-Band upconverter has an LO input frequency of 14 GHz, which is amplified, tripled in frequency to 42 GHz, amplified again, and then frequency doubled to 84 GHz. In the transmit mode, the upconverter module internally mixes the 8-12 GHz IF signal with the 84 GHz signal to produce a W-Band 92-96 GHz RF output signal.

In the receive mode, the HWIL upconverter module operates reciprocally where the 14 GHz signal is applied to the LO port and the W-Band signal (92-96 GHz) is applied to one of the RF ports. The RF input signal is provided by the forward-scattered energy (for bistatic receive) or by the back-scattered energy (for monostatic receive.) The HWIL upconverter module mixes a signal at six times the frequency of the LO signal (six times 14 GHz or 84 GHz) with the 92-96 GHz W-Band received signal at the RF port resulting in an 8-12 GHz IF data output signal. Some specifications of the SPACEK W-Band upconverter module are shown in Table 3.
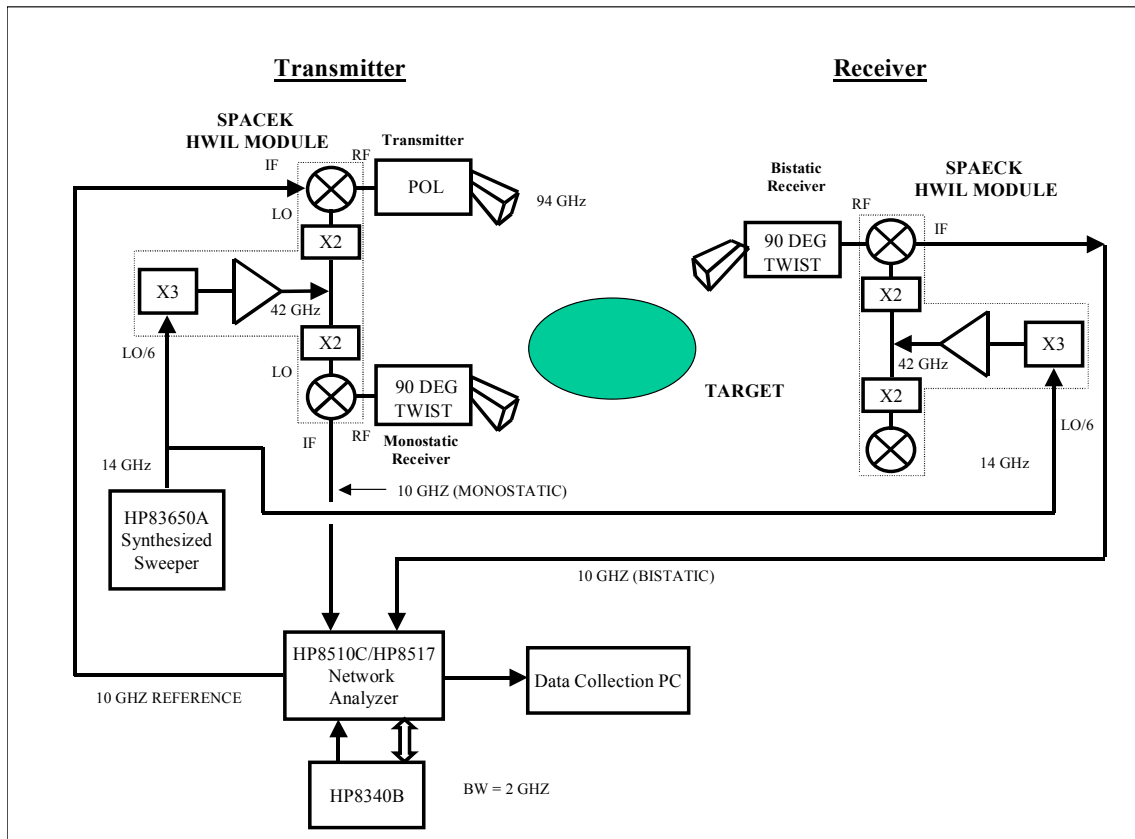
Figure 7. W-Band Measurement Instrumentation Overview

Table 3. Specifications of the SPACEK HWIL W-Band Upconverter

1. Operating Frequency	
LO/6	13.96 +/- 0.25 GHz
IF	10.24 +/- 1 GHz
RF	94.00 +/- 2 GHz
2. Maximum Conversion Loss	8 dB
3. Output Compression	1 dB Maximum, with 0 dBm IF Input

Even though the IF bandwidth was specified to be 2 GHz, the upconverter modules were shown to operate over a 4 GHz IF bandwidth.

C. RF System Parameters

General RF parameters for the transmitter and receiver chains are given as Tables 4 and 5.

Table 4. Initial Settings for the HP8510C Network Analyzer

Number of Points	201
Averaging	32
Power Level	8 dBm for W-band 0 dBm for Ka-band -8 dBm for X and Ku-bands
Frequency	8 to 12 GHz for W, Ka, and X-bands 14 to 18 GHz for Ku-band
Domain	Time
Time Gating	Off
S-Parameter	S21

Table 5. Transmitter Power and Antenna Gains

Frequency Band	Transmitter Power (dBm) Input to Tx Antenna	Transmitter and Receiver Antenna Gains (dB)
X	12	17
Ku	12	20
Ka	7	19.5
W	2	24

III. DATA COLLECTION METHODOLOGY

A. Calibration Procedures

Prior to collecting data at each frequency, the instrumentation was calibrated on an established reference point, such as a trihedral for monostatic, or on a direct path signal for bistatic. Calibration procedures were developed for both the monostatic and bistatic data collection sets. After the respective calibration procedure was conducted, then the actual monostatic or bistatic data was collected.

1. Monostatic Calibration

Prior to the monostatic calibration, the terrain turntable was covered with anechoic material. The transmit and the monostatic receive antenna (co-located with the transmit antenna) were set at a 45-degree depression angle. A trihedral was placed at the lower edge of the turntable and the transmit antenna was centered on it with the laser beam. The 201 points collected were then used to set the calibration reference for the actual data collection. The trihedral provided a large signal that provided a zero reference and a lower noise floor. Next, a 14-inch sphere was placed in the center of the anechoic covered turntable. The transmit antenna and monostatic receive antenna (co-located with the transmit antenna) were raised higher on the mast and pointed at the sphere. The reference sphere is known to have a –10 dBsm Radar Cross Section (RCS). The return from the sphere was the reference for the monostatic RCS calculations. The signal amplitude of the sphere, true to theory, varied little from frequency to frequency. The measured amplitude of the sphere was around -32.60 dB at each frequency relative to the reference trihedral. This value is relative to the calibration achieved with the trihedral. The terrain was then uncovered and smoothed and the backscattered signal amplitude and phase was collected at each depression angle.

Monostatic calibration was particularly challenging, and was ultimately fruitless at the Ku and X-Band frequencies. The reason that the monostatic calibration was more difficult was that the monostatic sand return is much lower than bistatic, and in fact, was not much higher than the system noise floor. In an early effort to obtain a good calibration set, a large 14-inch trihedral was used as the calibration standard. Eventually, it was determined that there was too much loss through the sand at the Ku and X-Band frequencies, since there was more penetration through the sand at these longer wavelengths. Therefore, it was not possible to obtain monostatic measurements at the two lower frequencies. However, at the W and Ka-Band frequencies, there was a strong signal peak for all of the measurements, and a good set of data was obtained for the monostatic case.

2. Bistatic Calibration

The process of calibration prior to the collection of bistatic data was very straightforward. The transmit and receive antennas were placed at a 0-degree depression angle and elevated to 12 feet. The terrain turntable was covered with anechoic material. In this configuration, the antennas were pointed directly at each other and provided a strong direct path signal that was used to calibrate the network analyzer. This set the calibration signal at 0 dB

amplitude and 0 degrees. The bistatic signal amplitudes collected were then relative to the direct path calibration signal.

B.   Data Collection Procedure

Data collection software was developed using the LabVIEW software package. A PC station was used to run the software that sent commands to the HP8510C Network Analyzer and the Turntable. Each data collection had the following sequence of events. The GUI screen allowed entry of the data filename and key information regarding the data to be collected. When the Run button was pushed, the first event was the collection of the time domain data from the HP8510C. When that was concluded, the operator then set the time gate around the return from the table, then set the domain to frequency and pushed the start button on the Turntable controller. From that point onward, 201 points over 4 GHz were collected at each 10-degree increment of the turntable, resulting in 36 data files. The average of each file was calculated and displayed immediately after collection, and the overall amplitude average of all of the 36 files over 360 degrees was calculated and displayed at the conclusion of the data collection. The next step of the process was calculating the sigma zero value for each frequency and for each depression angle.

IV. REFLECTIVITY ANALYSES

The bistatic RCS was derived using basic radar range equation principles. Expressions for the direct and bistatic signals were derived, then the ratio of the direct path signal to the reflected path signal was taken. The resulting expression removed the radar system dependencies, including any dependency on transmitted power. However, it is assumed that the transmit power level is the same for the direct path and bistatic path signals. The final equation solves for the reflectivity as a function of the direct path range, the bistatic path range, measured amplitude, and the area within the beam on the target, all of which are a function of geometry. Figure 8 shows the basic geometry from which the expressions were derived:
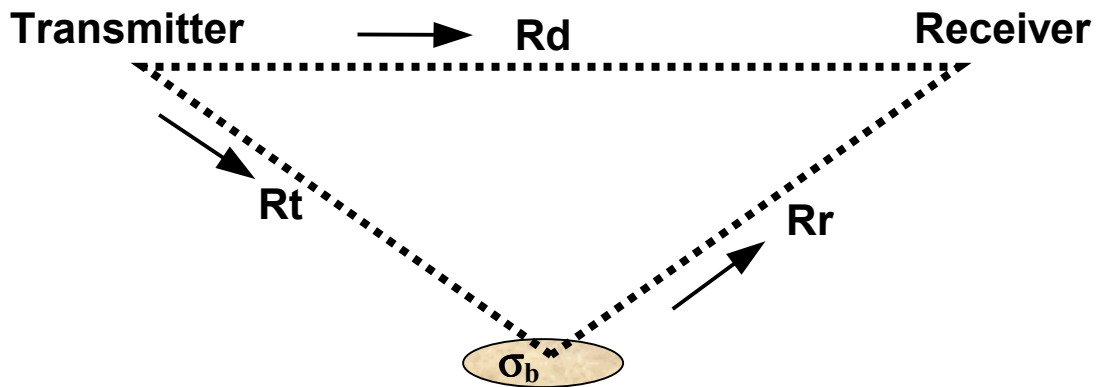

Figure 8. Illustration of Geometry of Bistatic Signal

where:

R_d = direct path range
R_t = range from transmit antenna to center of terrain sample
R_r = range from center of terrain sample to receive antenna
σ_b = bistatic reflectivity.

The expression for the direct path signal, S_d is:

$$S_d = (P_t G_t / 4(R_d^2)) \text{ x } (G_r \lambda^2 / 4\pi) \tag{1}$$

The expression for the bistatic path signal S_b, which was measured at different depression angles, is

$$S_b = (P_t G_t / 4\pi R_t^2) \text{ x } (\sigma_b / 4\pi R_r^2) \text{ x } (G_r \lambda^2 / 4\pi) \tag{2}$$

Taking the ratio of S_b to S_d, and, noting that S_d, the direct path calibration signal is 0 dB, or 1, then σ_b is solved through the following equation:

$$\sigma_b = S_b \, 4\pi \, R_b^4 / R_d^2 \quad \text{dBsm} \tag{3}$$

Then, relating the reflectivity to the physical area (A) over which the bistatic signal was measured, the final expression is

$$\sigma_o = \sigma_b / A \quad \text{dBsm/sm.} \tag{4}$$

V. MODELING

A simulation of the RF and millimeter wave environment has been implemented as a tool to help verify test results. Also the simulation allows for the formulation and testing of different models of relative clutter reflectivity, σ_0. Antenna pattern effects with respect to the finite clutter patch under test will be considered. The effort here is to keep the models as simple as possible while still obtaining results from the simulation that are a good match with the empirical data taken in the anechoic chamber.

In the clutter simulation, the reflection off of the clutter will be assumed to be specular; that is, the calculation of the received signal will be of the form

$$P_{rec} = \frac{P_t G_t G_r \lambda^2}{(4\pi)^3 R_t^2 R_r^2} \sigma_0 A_c \tag{5}$$

P_t = power transmitted
G_t = transmit antenna gain
G_r = receive antenna gain
λ = wavelength
R_t = range from transmitter to clutter
R_r = range from receiver to clutter
σ_0 = effective reflective area of clutter per unit area
A_c = physical area of clutter.

Generally, σ_o is modeled as a function of the relative angles from the transmitter to the clutter patch and the angle between the receiver and the clutter patch. Most often the depression angles from the transmitter and receiver to the clutter (Fig. 1) are used to model the clutter reflection magnitude. Also, the out-of-plane angle, or some variation of this, is used to indicate the receiver position with respect to the simple ray trace smooth surface reflection. Terms are also added to help simulate clutter surface roughness. Although much analysis has been done on the theory of clutter scattering, this simulation will simply implement one or more preexisting empirical models with the goal of eventually incorporating an original model. The primary model used during the early analysis is the Georgia Tech model [2]. It is not the intention of this work to perform an exhaustive verification of other models; however, a simple comparison of the empirical results with the simulation results utilizing these different models for clutter, σ_o, will be performed. The desire is to attempt to develop an independent empirical model that will provide a good match to the data. Initial results of the model [3] have matched the measured data quite well.

VI. REFLECTIVITY RESULTS FOR SAND

Figures 9 through 12 illustrate the complete set of data curves taken at each frequency. The first data collection at each frequency was at the in-plane position and at a 10-degree out-of-plane position. The data taken also included the 30-degree out-of-plane position. Three sets of bistatic data were collected at W-Band, two sets of bistatic data were taken at the other frequencies. The test plan is in the Appendix. A complete set of reflectivity curves for smooth sand from each of the data sets collected is shown on each graph. The complete set of in-plane co-pol reflectivity curves from each frequency is illustrated in Figure 13. Monostatic, or backscatter, reflectivity for W and Ka-Bands are shown in Figure 14. The monostatic reflectivity at Ka-Band is expected to be lower than at W-band; however, the measured values are lower than expected.

Since the antenna produced a fairly broad beam at each frequency [4], the in-plane and 10 degrees out-of-plane measurements were close in amplitude at all of the frequencies. The most consistent set of measurements were collected at W-Band. The reflectivity at W-Band was well behaved and very repeatable for each of the data collection sets taken. W-Band data was collected during the months of October 99, January 00, and June 00. The W-Band data curves for each in or out-of-plane measurement are nicely separated for each distinct geometry and polarization. The 30-degree out-of-plane measurement was more similar in value and curvature to the cross-pol measurements at all of the frequencies. The cross-pol results had lower amplitudes and are usually rather flat in character.

There is something quite interesting going on for the co-pol data at the 30-degree depression angle, especially at Ka, Ku and X-Bands. The bistatic signal intensity decreases to a minimum at 30 degrees and then increases. An experiment and analyses of this phenomenon was explored by Vanderford and Ferster [5] and determined to be a result of the Brewster angle effect. It was postulated that the lesser reduction in depth of the signal amplitude for W-Band at this angle might be due to the fact that the sand appears rough at the W-Band wavelengths.
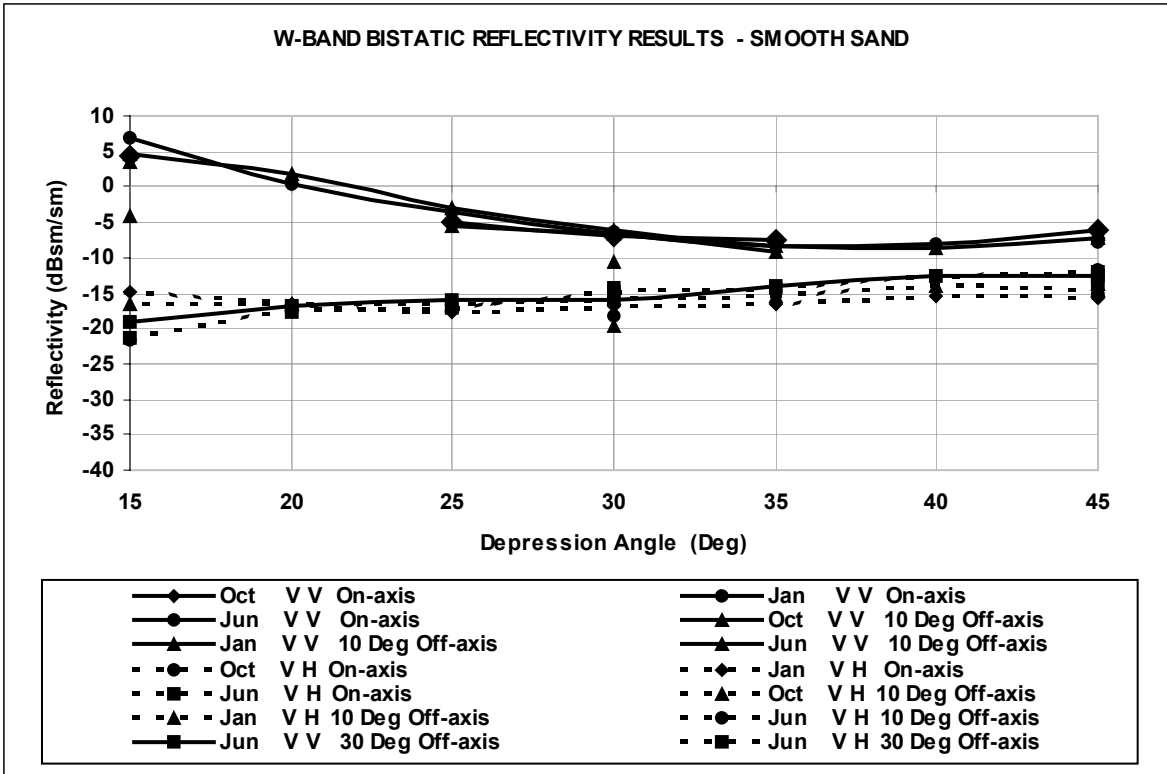
*Figure 9. W-Band Reflectivity Results for Smooth Sand*
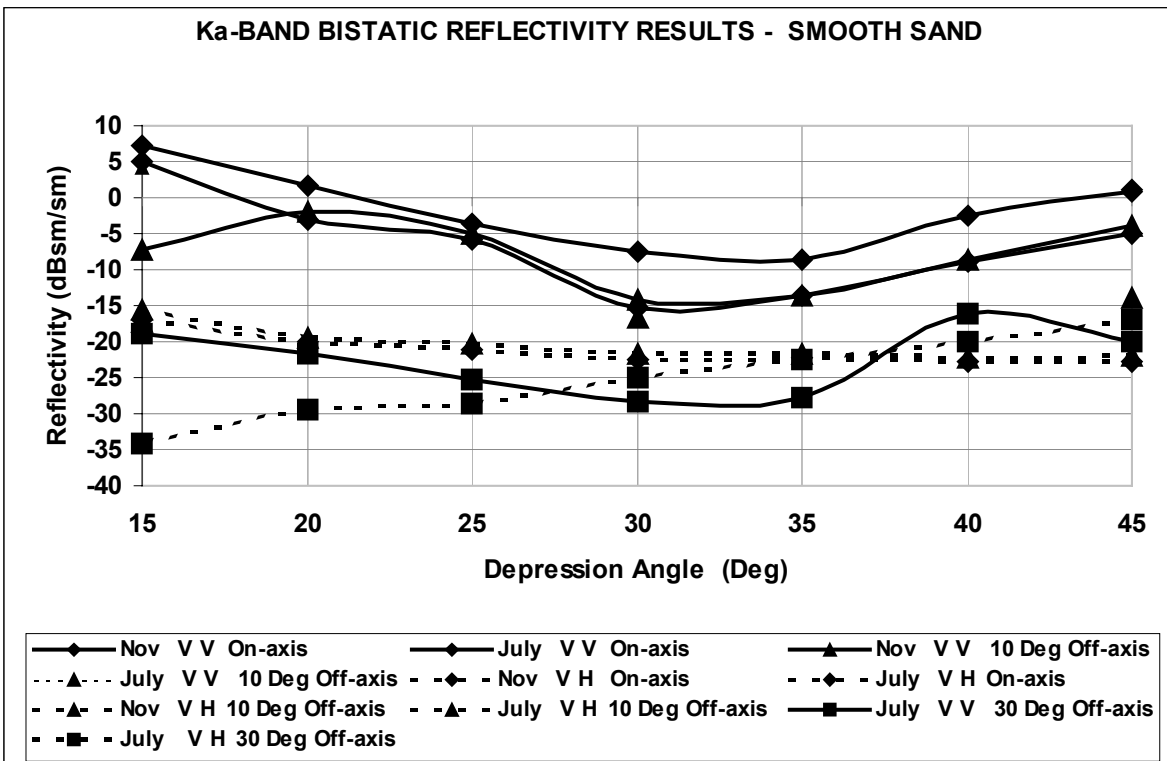
*Figure 10. Ka-Band Reflectivity Results for Smooth Sand*
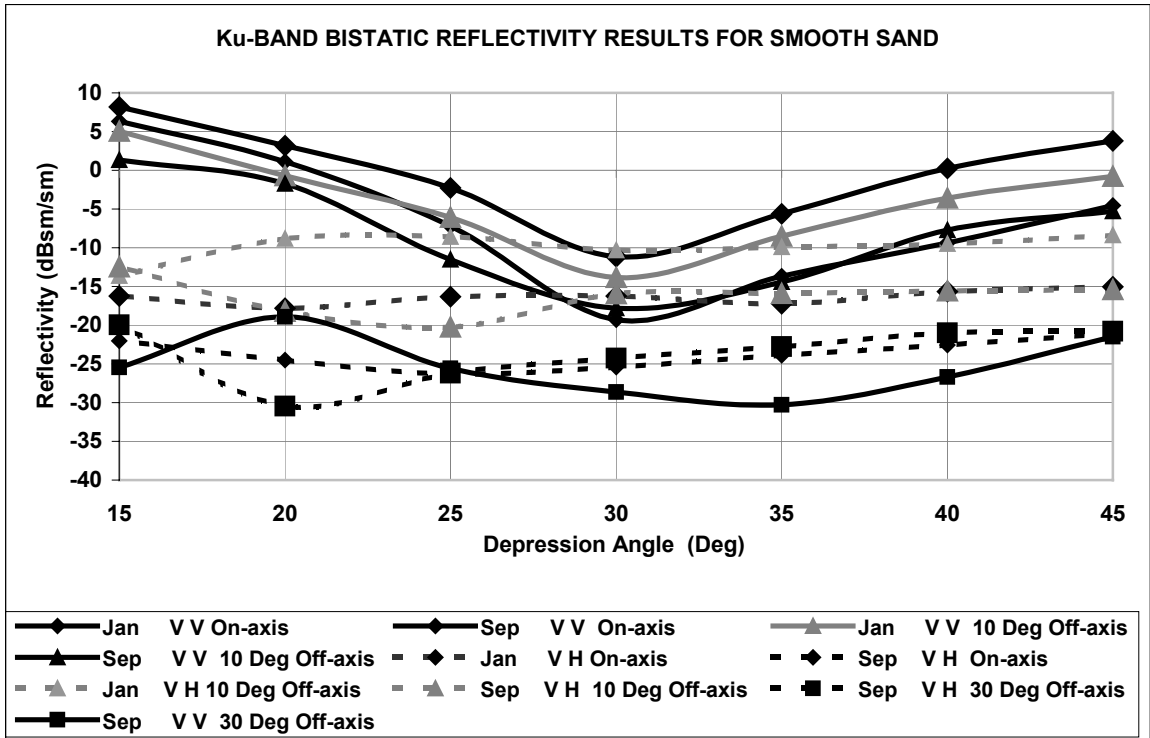
Figure 11. Ku-Band Reflectivity Results for Smooth Sand
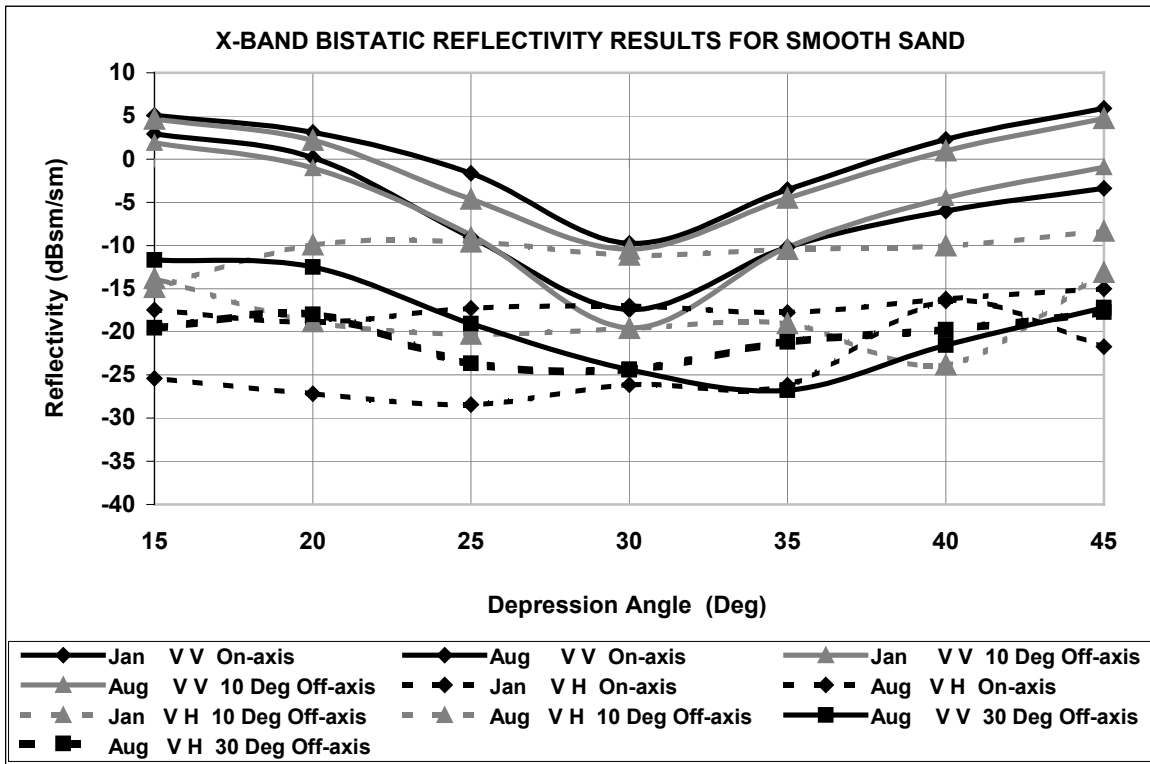
Figure 12. X-Band Reflectivity Results for Smooth Sand

16

SUMMARY OF BISTATIC REFLECTIVITY, V V, IN-PLANE, SAND

Legend: W Oct, W Jan, W Jun, Ka Nov, Ka July, Ku Jan, Ku Sep, X Jan, X Aug

X-axis: Depression Angle (15 to 45)
Y-axis: Reflectivity (dBsm/sm) (-40 to 10)
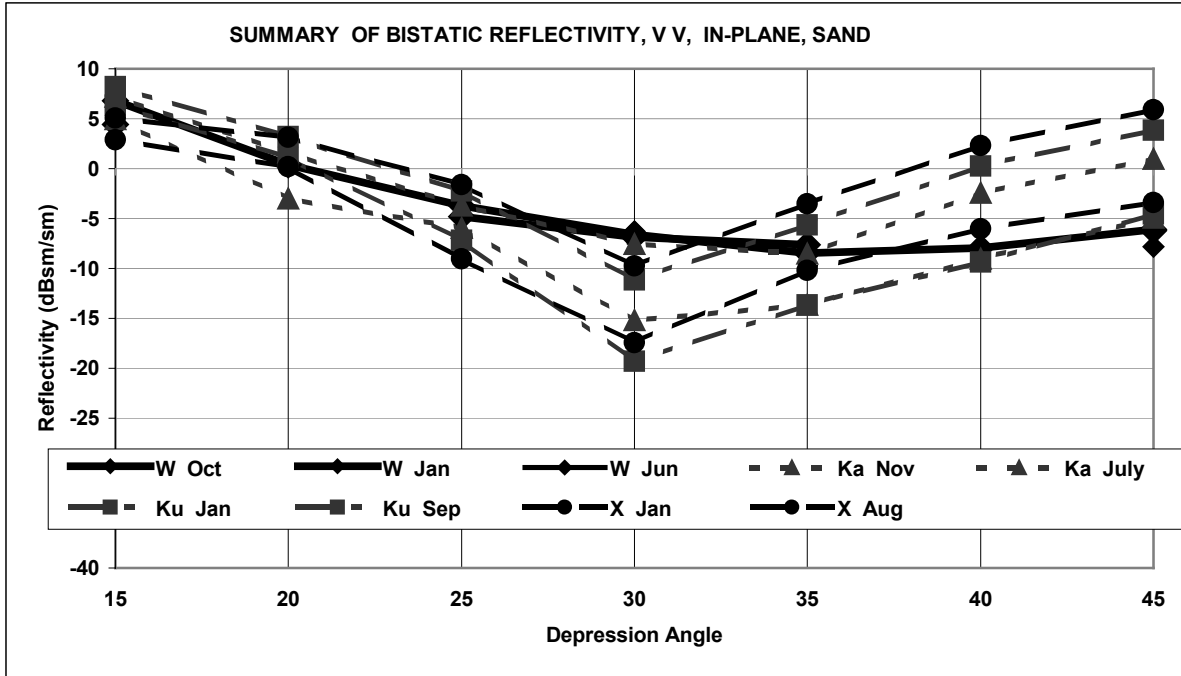
Figure 13. Summary of Co-Pol In-Plane Bistatic Reflectivity Results

Average Monostatic Reflectivity

Legend: W-Band, Ka-Band

X-axis: Depression Angle (Degrees) (15 to 45)
Y-axis: Reflectivity (dBsm/sm) (-35 to 0)
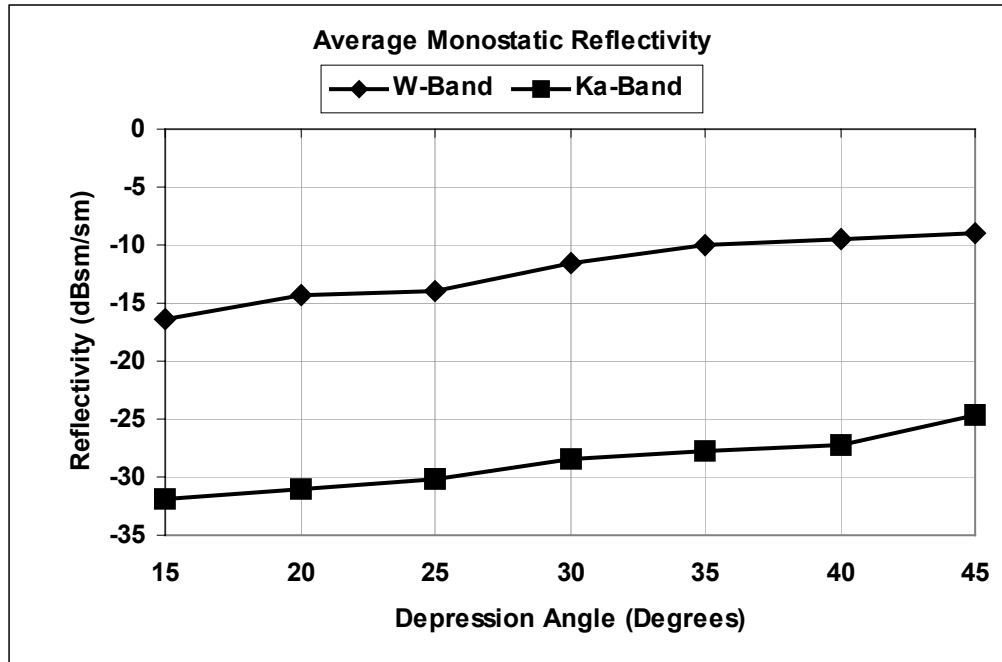
Figure 14. Average Monostatic Reflectivity for Ka and W-Band Over Smooth Sand

17

VII. SUMMARY

A complete set of bistatic data has been collected at each frequency and monostatic data at Ka and W-Bands. Overall, the facility has provided repeatable measurements for each of the data sets collected, and the data collection and reduction methodologies have been refined. Current data analysis efforts focus on completion of models and simulation of the empirical data and on completion of the probability density function analyses. Future plans include collection of reflectivity data from flat plates, rough rocky terrain, and grass sod terrain.

REFERENCES

1.   Willis, Nicholas J., "Bistatic Radar," chap 25 in Skolnik, M. I. (ed): Radar Handbook, McGraw-Hill, Inc., New York, 1990, pp 25.18-25.21.

2.   Currie, Nicholas C. and Brown, Charles E., Principles and Applications of Millemeter-Wave Radar, Artech House, 1987.

3.   Matkin, et.al., Proceedings of the 2001 IEEE Radar Conference, May 2001.

4.   Matkin, et.al., Proceedings of the Multi/Hyperspectral Sensors, Measurements, Modeling and Simulation Workshop, Nov. 2000.

5.   Vanderford, Perry J., and Ferster, Tommy J., "Study of Brewster Angle on Sand Terrain in Bistatic Reflectivity Measurement Facility," Technical Report CR-RD-SS-00-07.

APPENDIX
TEST PLAN

The test plan is illustrated in Figure A-1. A complete set of 36 data files was collected at each depression angle for V V and then for V H polarizations at each of three different positions of in-plane, 10 and 30 degrees out-of-plane.

Bistatic Measurements (W, Ka, Ku, X)									
Receiver Position	**Polarization**	**Depression Angle (Degrees)**							
		45	40	35	30	25	20	15
In-plane	V V	▲	▲	▲	▲	▲	▲	▲
	V H	▲	▲	▲	▲	▲	▲	▲
10 Degrees Out-of-plane	V V	▲	▲	▲	▲	▲	▲	▲
	V H	▲	▲	▲	▲	▲	▲	▲
30 Degrees Out-of-plane	V V							
	V H	▲	▲	▲	▲	▲	▲	▲
Monostatic Measurements (W, Ka)								
In Plane	V V	▲	▲	▲	▲	▲	▲	▲

INITIAL DISTRIBUTION LIST

		Copies
IIT Research Institute ATTN: GACIAC 10W. 35th Street Chicago, IL 60616		1
Defense Technical Information Center 8725 John J. Kingman Rd., Suite 0944 Ft. Belvoir, VA 22060-6218		1
Sensors Directorate, Electromagnetic Scattering Branch ATTN: Bertus Weijers 80 Scott Drive Hanscom AFB, MA 01731-2909		1
Simulation Technologies, Inc. ATTN: Perry J. Vanderford Suite 4 3307 Bob Wallace Ave. SW Huntsville, AL 35805		2
AMSAM-RD,	Mr. Mike Schexnayder	1
AMSAM-RD-AS-I-RSIC		2
AMSAM-RD-AS-I-TP		1
AMSAM-RD-MG,	Dr. Robin Bucklew Dr. Jay Loomis Mr. Gerald E. Scheiman	1 1 1
AMSAM-RD-MG-RF,	Ms. Brenda L. Matkin Mr. James H. Mullins	6 4
AMSAM-RD-SS-HW,	Mr. Alex Jolly	1
AMSAM-RD-SE,	Mr. Tommy J. Ferster	2
AMSAM-L-G-I,	Mr. Fred Bush	1
SFAE-AMD-LT-MEADS,	Mr. Edward Manlove	1